

Highly anisotropic Bose-Einstein condensates: crossover to lower dimensionality

Kunal K. Das

Optical Sciences Center and Department of Physics, University of Arizona, Tucson, AZ 85721 and
Department of Physics and Astronomy, SUNY, Stony Brook, NY 11794-3800*

(Dated: October 26, 2018)

We develop a simple analytical model based on a variational method to explain the properties of trapped cylindrically symmetric Bose-Einstein condensates (BEC) of varying degrees of anisotropy well into regimes of effective one dimension (1D) and effective two dimension (2D). Our results are accurate in regimes where the Thomas-Fermi approximation breaks down and they are shown to be in agreement with recent experimental data.

PACS numbers: 03.75.Fi, 05.30.Jp, 67.40.Db, 03.65.Ge

I. INTRODUCTION

There has been a growing interest in Bose Einstein condensation in effective lower dimensions, with experimental realization finally becoming reality [1]. Apart from the purely academic interest, there is a very practical interest as well arising from the rapidly developing endeavor to create efficient atom waveguides with potential applications in interferometry and gyroscopes. For trapped gases effective lower dimensionality means that excitations along the tightly confined dimension(s) are energetically not allowed. This is a limiting case of highly anisotropic condensates which are becoming more common with a new generation of BEC experiments on surface micro traps [2, 3].

Interest in condensates of extreme anisotropy is evident in numerous current theoretical and experimental work on atomic waveguides, quasi-2D configurations [4, 5] and the Tonks-Girardeau (TG) 1D limit [6, 7, 8] in which impenetrable bosons show fermionic properties. Magnetic waveguides for neutral atoms of diverse design have been constructed in many laboratories [3, 9, 10, 11, 12, 13]. Bessel beams [14] have been used to produce wave-guide-like optical confinement. With a slight longitudinal potential these waveguides can be treated as high aspect ratio traps. Atoms have been trapped in a 2D optical lattice consisting of quasi-1D optical wells [15] each with an aspect ratio of up to about 2000. Work is underway at JILA on various waveguide and near-waveguide configurations [16]. On the theoretical side the various regimes of quantum degeneracy in both the 1D and 2D limits have been studied in detail in several recent papers [17, 18, 19, 20, 21, 22, 23, 24, 25, 26].

But a simple model is lacking which would describe how a condensate changes as it becomes more anisotropic and eventually crosses over to effective lower dimensionality. For condensates in 3D, of atoms with positive scattering length, a highly effective and yet essentially simple analytic description was achieved through the Thomas-Fermi Approximation (TFA) [27]. It neglects the kinetic

energy in the Gross-Pitaevskii (GP) equation which is the mean-field description of the condensate and it is justified for large condensates with aspect ratios of the order of unity. But as the aspect ratio deviates farther from unity, the kinetic energy in the constricted direction becomes increasingly more important and the TFA does not work so well. Although there have been numerous, insightful refinements of the TFA [28, 29, 30, 31, 32] they do not directly improve on it for highly anisotropic BEC. It is desirable to have a theoretical model comparable to the TFA in simplicity but one which is successful in describing condensates from the 3D regime with increasing degree of anisotropy all the way to regimes of effective lower dimensionality. That is the objective of this paper.

For longitudinally homogeneous systems, we have recently coauthored a study of the crossover from 3D to effective 1D [33]. Here we will consider gases harmonically confined in all directions and a crossover to effective 2D as well. We will use a variational approach to obtain analytic expressions for the chemical potential, total energy, release energy and also the energy spectrum valid over a wide range of parameters that include the regime of crossover to lower dimensions. In Sec. II we compare our chemical potential with accurate numerical solutions of the GP equation and the Thomas-Fermi expression and then in Sec. III we discuss the crossover regime. In Sec. IV we compare the release energy from our model with experimental data from Ref. [1]. Then in Sec. V we consider the Bogoliubov equations for quasiparticle excitations and obtain the energy spectrum for geometries close to effective 1D and 2D.

II. CHEMICAL POTENTIAL

At zero temperature in the lowest order mean-field approximation the condensate is described by the wave function that minimizes the GP energy functional [27] which in cylindrical co-ordinates is

$$E[\Phi] = N\hbar\omega \int r dr \int dz \left[\frac{\gamma^{1/3}}{2} (|\nabla_r \Phi|^2 + r^2 |\Phi|^2) + \frac{\gamma^{-2/3}}{2} (|\partial_z \Phi|^2 + z^2 |\Phi|^2) + Ng|\Phi|^4 \right]. \quad (1)$$

*Present address

We have defined the aspect ratio as the ratio of the radial and the axial trapping frequencies $\gamma = \omega_r/\omega_z$. The interaction strength is determined by the scaled scattering length $g = a/a_0$ and by the atom number N which we take to be equal to the condensate number assuming temperatures close to absolute zero. The co-ordinates r and z are scaled by the respective oscillator lengths $r_0 = \sqrt{\hbar/m\omega_r}$ and $z_0 = \sqrt{\hbar/m\omega_z}$, with the mean oscillator length $a_0 = \sqrt{\hbar/m\omega}$ being defined by the geometric mean frequency, $\omega = (\omega_r^2\omega_z)^{1/3}$. The condensate wavefunction is $(e^{-im\theta}/\sqrt{2\pi})\Phi(r, z)$ with $m = 0$ and normalization $\int r dr \int dz |\Phi(r, z)|^2 = 1$.

Functional minimization $\delta E/\delta\Phi = 0$ with the normalization condition gives the GP equation

$$\frac{\gamma^{1/3}}{2} (-\nabla_r^2 + r^2) + \frac{\gamma^{-2/3}}{2} (-\partial_z^2 + z^2) + 2Ng|\Phi|^2 = \frac{\mu}{\hbar\omega}. \quad (2)$$

This determines the optimum condensate wavefunction Φ and the corresponding chemical potential μ . For condensates with all its spatial dimensions of comparable magnitudes the Thomas-Fermi approximation provides a accurate value of the chemical potential

$$\mu_{TF} = \frac{\hbar\omega}{2} (15Ng)^{2/5}. \quad (3)$$

This expression has no dependence on the aspect ratio, whereas we would expect the chemical potential to change as the aspect ratio changes. In order to obtain analytic expressions for Φ and μ that will have the correct dependence on the aspect ratio we take a variational approach with a trial wavefunction containing a few parameters and then minimize the energy functional with respect to them [34]. In choosing our trial function we note that for highly anisotropic traps, in the direction of weak confinement the condensate size far exceeds the oscillator length and the kinetic energy (which scales as the inverse square of the size) becomes negligible, so a Thomas-Fermi form is appropriate. In the squeezed coordinate the interaction term has lesser relative importance so that a Gaussian form is suitable.

A. Cigar Geometry

For the cigar geometry with $\gamma \gg 1$, we take our normalized trial function to be

$$\Phi_{\text{cigar}}(r, z) = \left(\frac{3\beta_r}{2d^3}\right)^{1/2} e^{-\beta_r r^2/2} \sqrt{d^2 - z^2} \Theta(d^2 - z^2), \quad (4)$$

where β_r and d are variational parameters and $\Theta(x)$ is the unit step function. In evaluating the energy functional, Eq. (1), for this trial function, we recognize that the kinetic energy in the transverse direction should be included, but not that in the axial direction. We thus obtain

$$\frac{E[d, \beta_r]}{N\hbar\omega} = \left[\frac{\gamma^{1/3}}{2} \left(\beta_r + \frac{1}{\beta_r} \right) + \frac{\gamma^{-2/3}d^2}{10} + \frac{3\beta_r Ng}{5d} \right]. \quad (5)$$

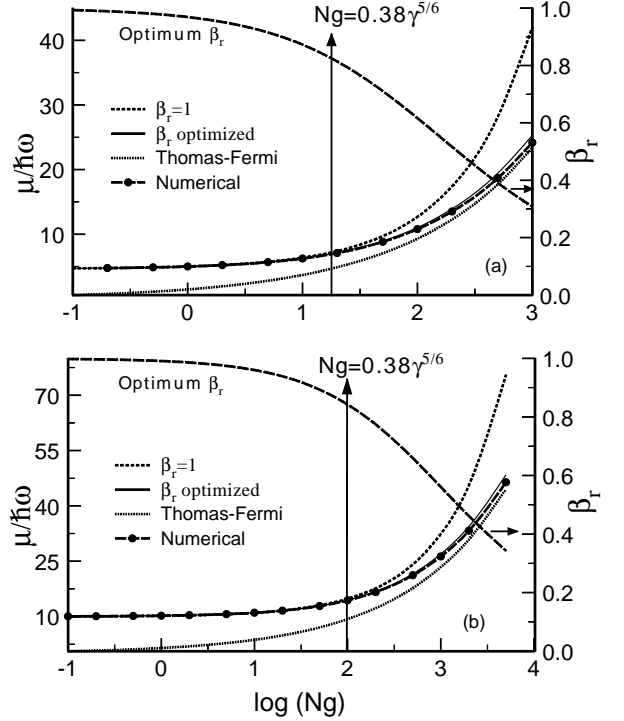


FIG. 1: Comparison of chemical potential obtained from various approaches, for cigar-shaped traps with (a) $\gamma = 100$ and (b) $\gamma = 1000$. The methods are numerical solution of the Gross-Pitaevskii equation; the Thomas-Fermi approximation; analytic expression Eq. (7) with optimized β_r and d ; and the same with $\beta_r = 1$. The optimum value of β_r is plotted with the right axis scale.

Minimizing E with respect to d and β_r gives

$$d^3 = 3\beta_r Ng \gamma^{2/3}; \quad \frac{1}{\beta_r^2} = 1 + \frac{6Ng}{5d} \gamma^{-1/3}. \quad (6)$$

These coupled equations can be easily solved numerically, and the chemical potential corresponding to the optimum parameters is

$$\begin{aligned} \mu &= \hbar\omega \left[\frac{\gamma^{1/3}}{2} \left(\beta_r + \frac{1}{\beta_r} \right) + \frac{1}{2} \left(\frac{3\beta_r Ng}{\gamma^{1/3}} \right)^{2/3} \right] \\ &= \frac{\hbar\omega_r}{2} \left(\beta_r + \frac{1}{\beta_r} \right) + \frac{1}{2} (3\beta_r N a \omega_r \omega_z \hbar \sqrt{m})^{2/3}. \quad (7) \end{aligned}$$

This satisfies the thermodynamic relation $\mu = \partial E/\partial N$ as expected. It is apparent from the unscaled form that the last term is $\propto \omega_z^{2/3}$ and hence vanishes in the limit $\omega_z \rightarrow 0$, also in that limit $\beta_r \rightarrow 1$ so that the chemical potential μ equals the transverse ground-state energy $\hbar\omega_r$ as we would expect. In fact for very elongated traps, to a very good approximation we can set $\beta_r = 1$ and Eq. (7) reduces to a self-contained analytic expressions for μ dependent only on N, a and γ all of which are measurable parameters of the system.

In order to test the accuracy and validity of our approximation we compare the analytic expressions for the chemical potential with accurate numerical solutions of the GP equation, obtained using a discrete variable representation (DVR) mesh in r (Laguerre DVR) and z (Hermite DVR) [35, 36, 37]. We checked for convergence of the numerical results as a function of mesh size and range. Typically, 1,000 to 1,500 mesh points sufficed.

In Fig. 1 we plot the chemical potential computed in various ways for cigar traps of two different aspect ratios. It is clear that the variational chemical potential using expression (7) with optimized β_r closely follows the numerically computed chemical potential over a large range of Ng . For low linear densities, the expression with $\beta_r = 1$ is sufficient but it fails as the density increases. On the other hand the Thomas-Fermi expression (3) is accurate at high densities and breaks down at low densities since it approaches zero while the correct μ should approach the zero-point energy.

B. Pancake Geometry

On carrying through a similar analysis for the pancake geometry with $\gamma \ll 1$, taking as trial function

$$\Phi_{\text{pan}} = \frac{2}{b^2} \left(\frac{\beta_z}{\pi} \right)^{1/4} (b^2 - r^2)^{1/2} e^{-\beta_z z^2/2} \Theta(b^2 - r^2), \quad (8)$$

we find that the energy functional, neglecting the transverse kinetic energy, is

$$\frac{E[b, \beta_z]}{N\hbar\omega} = \left[\frac{\gamma^{1/3} b^2}{6} + \frac{\gamma^{-2/3}}{4} \left(\beta_z + \frac{1}{\beta_z} \right) + \frac{8Ng}{3b^2} \sqrt{\frac{\beta_z}{2\pi}} \right]. \quad (9)$$

The equations for the optimum parameters that minimize the energy are

$$b^4 = 16 \frac{Ng}{\gamma^{1/3}} \sqrt{\frac{\beta_z}{2\pi}}, \quad \frac{1}{\beta_z^2} = 1 + \frac{16 Ng \gamma^{2/3}}{3b^2 \sqrt{2\pi\beta_z}}, \quad (10)$$

and the corresponding expression for the chemical potential

$$\mu = \hbar\omega \left[\frac{\gamma^{-2/3}}{4} \left(\beta_z + \frac{1}{\beta_z} \right) + \left(\frac{8\beta_z}{\pi} \right)^{1/4} \sqrt{Ng\gamma^{1/3}} \right]. \quad (11)$$

As we did for the cigar geometry, we plot the chemical potential evaluated in various ways in Fig. 2. The deviation of the Thomas-Fermi expression from the correct expression for μ is more pronounced in this geometry while our variational expression from Eq. (11) reproduces almost exactly the numerical solution of the GP equation over the range of Ng shown. Even the analytic expression for μ with $\beta_z = 1$ is accurate to large values of Ng . The reason for the better agreement is larger relative importance of the kinetic energy in the tightly confined direction. Note also that in both Fig. 1 and Fig. 2, differences between the TFA and the numerical results persist to larger

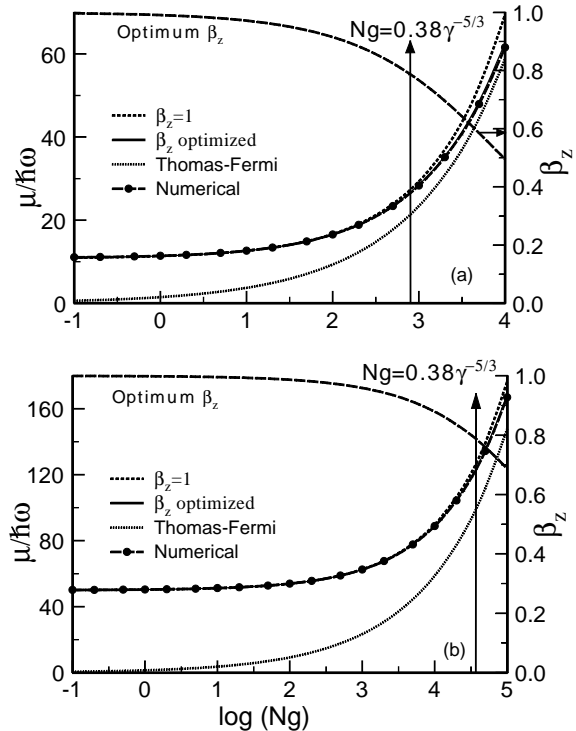


FIG. 2: The chemical potential for pancake shaped traps obtained from various approaches, for aspect ratios (a) $\gamma = 0.01$ (top) and (b) $\gamma = 0.001$. In both cases, the result with optimized b and β_z is essentially indistinguishable from the numerical solution of the GP equation.

values of Ng as the anisotropy increases i.e. γ deviates more from unity.

In Fig. 3 we plot the chemical potential obtained from our variational expressions in Eqs. (7) and (11) as a function of the aspect ratio γ , over several orders of magnitudes that vary from very elongated cigar condensates to extremely oblate pancake shapes. Strong variation with the aspect ratio is apparent. In the same figure the Thomas-Fermi chemical potential μ_{TF} (3) appears as flat horizontal lines tangential at $\gamma = 1$ to the lines corresponding to our calculated μ . Thus our expressions for the chemical potential agree with the Thomas-Fermi value for spherical symmetry.

III. CROSSOVER TO LOWER DIMENSIONS

The variational parameters we have used to obtain the chemical potential also provide a measure of the effective dimensionality of the condensate. A trapped Bose gas is considered to be in effective lower dimension if excitations in the tightly confined dimension are frozen. Thus a criteria for crossover to lower dimensionality [1] is when the interaction energy per particle is comparable to the energy ($\sim \hbar\omega_{\text{tight}}$) to excite the first excited mode

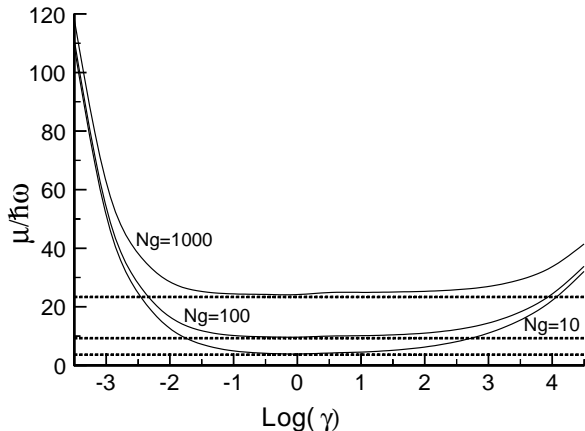


FIG. 3: The variationally optimized chemical potential μ is plotted as a function of the aspect ratio γ for different mean field strengths. For $\gamma > 1$ Eq. (7) is used and for $\gamma < 1$ Eq. (11). The horizontal dashed lines, that represent the Thomas-Fermi chemical potential μ_{TF} , are tangential to the corresponding variational μ at their lowest points at $\gamma = 1$.

in the tightly confined direction. For a weakly interacting Bose gas at low densities the interaction energy is roughly equal to the Thomas-Fermi or 3D chemical potential so that the condition for lower dimensionality is $\mu_{TF} < \hbar\omega_{tight}$ which in our units become

$$gN_{1D} < \sqrt{\frac{32}{225}} \gamma^{5/6} \simeq 0.38 \times \gamma^{5/6}$$

$$gN_{2D} < \sqrt{\frac{32}{225}} \gamma^{-5/3} \simeq 0.38 \times \gamma^{-5/3}. \quad (12)$$

In Figs. 1 and 2, we have plotted the optimum value of β_r and β_z respectively along the right axis. The values corresponding to the crossover to one dimension $gN_{1D} = 0.38\gamma^{5/6}$ and to two dimension $gN_{2D} < 0.38\gamma^{-5/3}$ are indicated. We see that this roughly corresponds to $\beta_r \sim 0.8$ and $\beta_z \sim 0.8$. Thus the values of β_r and β_z give a measure of the dimensionality of the system: when $\beta_r \sim 1$ the system is effectively one-dimensional since the transverse profile of the condensate coincides with that of the transverse ground state, likewise when $\beta_z \sim 1$ the system is effectively two dimensional. As these parameters deviate from unity the system approaches 3D. It is worth noting at this point that in Ref. [33] a similar criterion was used to study the 1D-3D crossover for a homogeneous system, although the parameter used was different, being the effective 1D interaction strength.

The 1D case is of particular interest because at extreme low density and tight confinement the gas becomes an impenetrable Tonks-Girardeau gas [6, 7]. That regime is a subset of the regime of one-dimensionality. A wavefunction for a gas of such impenetrable bosons can be mapped to that of a gas of free fermions.

With slight rearrangement the criterion (12) we have used above for one dimensionality can be written as

$N < 0.38 \times (r_0/a)\gamma$. The impenetrable regime requires a much more stringent condition $k_F r_0^2/a \ll 1$ [17], where k_F is the Fermi wavevector of the equivalent Fermi system. For a large enough number of atoms and at zero temperature, the asymptotic form of the harmonic oscillator modes provides an estimate for the Fermi wavevector $k_F = \sqrt{2N}/z_0$, so that the condition for an impenetrable gas translates to $N \ll \frac{1}{2}\gamma(a/r_0)^2$. For typical traps $a \ll r_0$ which means that the particle number needs to be much smaller than that required for one-dimensionality. Thus it follows from our considerations above that the transverse profile in the impenetrable regime has to be that of the ground state of the transverse trap potential.

Our variational functions however cannot be applied to the Tonks-Girardeau regime, since the Thomas-Fermi profile in the axial direction has to be replaced by a square-root of a parabola [18], and the axial energy is simply the Fermi energy for N particles in 1D. Thus while the energies and chemical potential we have derived can be applied over a wide range of parameters spanning effective 1D and 2D, they are not meant to describe the impenetrable regime.

IV. COMPARISON WITH EXPERIMENT

In the experiment in Ref. [1] where BEC in effective lower dimensions was achieved, the crossover from a 3D to lower dimensionality was deduced (i) by observing a sudden change in the aspect ratio of the released condensate when the number of atoms was lowered below a certain value, and (ii) by observing a saturation of the release energy at the zero-point kinetic energy in the tightly confined direction. Since the measurement of the aspect ratio was done several milliseconds after release from the trap, a proper theoretical description would involve the dynamics [38] of the expansion of the condensate which we do not consider in this paper. However due to conservation of energy we can estimate the release energy in our model and compare it with the experimentally observed values.

The release energy is the energy of the system after the traps are switched off, which is just the sum of the kinetic and the interaction energies of the condensate before release. For the cigar geometry $\gamma \gg 1$, the variational calculation in Sec. II gives the release energy per particle

$$E_{\text{rel}} = \frac{\hbar\omega_r\beta_r}{2} + \frac{\hbar\omega_z d^2}{5}, \quad (13)$$

where we use the optimized parameters β_r and d from Eq. (6). The release energy in [1] is plotted as a function of the half-length (Z) of the condensate. It turns out that the axial expansion in the 1D experiment was negligible within the time of flight till measurement so that for comparison we simply need the initial half-length before release.

Considering the form of our trial function (4) it is tempting to identify d as the half-length of the con-

densate. However, this would not be correct since the trial function assumes a *uniform* cylindrical cross-section along the length of the condensate, whereas as we approach the 3D regime, the condensate tends to be an ellipsoid, so that the center will tend to bulge out more than the ends.

One could invoke arguments based on geometry to extract the half length from our expression for d . However a much easier way to do that is to make sure that our expression for the half-length has the correct form in the 1D limit and the 3D (Thomas-Fermi) limit

$$Z_{1D} = z_0 \left[3Ng\gamma^{2/3} \right]^{1/3}, \quad Z_{3D} = z_0 \left[15Ng\gamma^{5/3} \right]^{1/5}. \quad (14)$$

The 1D limit is obtained trivially $d(\beta_r = 1) \rightarrow Z_{1D}$. In considering the 3D limit we note that $1/\sqrt{\beta_r}$ is the width of transverse variational profile, and the second term in the expression (6) for β_r measures the deviation from 1D; as the condensate moves away from the 1D regime and approaches a ellipsoidal shape, that deviation would be maximum at the center and negligible at the end. Thus we take an average value for the deviation and define the modified parameter $\bar{\beta}_r$.

$$\frac{1}{\bar{\beta}_r^2} = 1 + \frac{3Ng}{5d}\gamma^{-1/3} \quad (15)$$

It is easy to see that in the 3D limit $\bar{\beta}_r \ll 1$, we have $\bar{\beta}_r^2 \simeq 5d\gamma^{1/3}/3Ng$ and we get the correct limit $d(\bar{\beta}_r) \rightarrow Z_{3D}$, while we get the correct 1D limit as well $d(\bar{\beta}_r = 1) \rightarrow Z_{1D}$. Thus in the intermediate regime we expect the half-length to be given to a good approximation by

$$Z = 3Ng\bar{\beta}_r\gamma^{2/3}. \quad (16)$$

We stress that the release energy should be evaluated with the optimized variational parameters from Eq. (6). The variational process optimizes energy and not condensate dimensions and hence there is no inconsistency. In Fig. 4 we plot the release energy per particle from Eq. (13) versus the half length from Eq. (16) for the parameters corresponding to the 1D experiment in Ref. [1]: sodium atoms in a magnetic trap with radial frequency $\omega_r = 2\pi \times 360$ Hz and axial frequency $\omega_z = 2\pi \times 3.5$ Hz, so that the aspect ratio is $\gamma \simeq 103$. A comparison with plot (3b) presented in Ref. [1] shows that our expression for the release energy closely follows their measured data for the release energy; as the system approaches effective 1D the saturation of the release energy at the radial zero-point energy is clear.

In the pancake geometry the release energy per particle from our variational calculations is

$$E_{\text{rel}} = \frac{\hbar\omega_z\beta_r}{4} + \frac{\hbar\omega_r b^2}{6} \quad (17)$$

Considering the agreement in the cigar case we expect this expression to agree well with experimentally measured release energy in this geometry. We will not do an

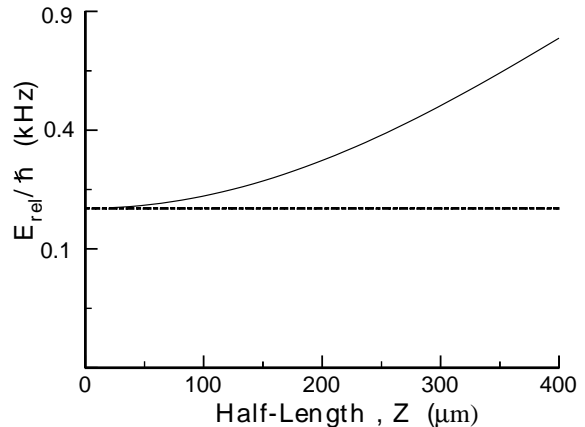


FIG. 4: The release energy per particle E_{rel}/\hbar plotted as a function of the half-length of a cigar-shaped condensate of trapping frequencies $\omega_r = 2\pi \times 360$ Hz and $\omega_z = 2\pi \times 3.5$ Hz. Compare with Fig. 3(b) in Ref. [1]. The horizontal line represents the transverse zero-point energy.

actual comparison here for two reasons: First the above expression is for strictly cylindrical geometry whereas the trap configuration in the 2D experiment in [1] was not. Secondly unlike the 1D experiment there is significant expansion of the condensate in all directions till the time of measurement which involves the dynamics of expansion which is not a topic of this paper.

V. EXCITED STATES

In Sec. II we found the chemical potential to be increasingly different from the Thomas-Fermi value as the anisotropy of the system increases; since the quasiparticle spectrum depends on the chemical potential we should expect some consequent changes. The energy spectra for purely 1D and 2D system have been known for sometime [22], also solutions have been found for cylindrical geometry in 3D using TFA in all directions [39, 40, 41]. We will consider here how the spectrum changes as the system deviates from effective 1D or 2D.

Consider the Bogoliubov equations for the quasiparticle excitations; as with the ground state we assume factorized spatial dependence of the quasi-particle modes $U(r, z)$ and $V(r, z)$. We first discuss the pancake geometry. The strong axial confinement makes it reasonable to assume that U, V have the same z -dependence as the condensate:

$$U_{nm}(r, z) = R_{nm}^+(r)\zeta(z), \quad V_{nm}(r, z) = R_{nm}^-(r)\zeta(z), \\ \Phi(r, z) = \phi(r)\zeta(z) \quad \text{with} \quad \zeta(z) = \left(\frac{\beta_z}{\pi}\right)^{1/4} e^{-\beta_z z^2/2}. \quad (18)$$

This allows us to integrate out the axial dependence. On using our expression Eq. (11) for the chemical potential

the terms reflecting axial kinetic and potential energy drop out both in the GP and the Bogoliubov equations and they take the form

$$\begin{aligned} & [-\nabla_r^2 - (b^2 - r^2) + 4g_{2D}|\phi|^2] \phi = 0 \\ & \left[-\nabla_r^2 - (b^2 - r^2) + \frac{m^2}{r^2} + 8g_{2D}|\phi|^2 \right] R_{nm}^\pm \\ & + 4g_{2D}|\phi|^2 R_{nm}^\mp = \pm 2 \epsilon_{nm} R_{nm}^\pm, \quad (19) \end{aligned}$$

Here $g_{2D} = b^4/16$ defines an effective transverse two-body interaction strength and $\hbar\omega_r\epsilon_{nm}$ are the transverse normal mode energies.

The sum and difference of the Bogoliubov equations can be converted to normal mode equations for the transverse density and phase fluctuations

$$\begin{aligned} & \left[-\frac{\nabla_r}{|\phi|^2} [|\phi|^2 \nabla_r] + \frac{m^2}{r^2} + 4g_{2D}|\phi|^2 \right] \frac{\rho_{nm}}{\rho_0} = 4i \epsilon_{nm} \theta_n \\ & \left[-\frac{\nabla_r}{|\phi|^2} [|\phi|^2 \nabla_r] + \frac{m^2}{r^2} \right] \theta_{nm} = -i \epsilon_{nm} \frac{\rho_{nm}}{\rho_0}. \quad (20) \end{aligned}$$

This is achieved by writing the small amplitude fluctuations of the condensate wavefunction as $\delta\phi = \sqrt{\rho}e^{i\delta\theta} - \sqrt{\rho_0}$ about its equilibrium $\phi_0 = \sqrt{\rho_0}$, whereby we get the well known forms for the linearized density and phase fluctuations [42]

$$\delta\rho = \sqrt{\rho_0}(\delta\phi + \delta\phi^*) \quad \delta\theta = \frac{-i}{2\sqrt{\rho_0}}(\delta\phi - \delta\phi^*) \quad (21)$$

and the corresponding normal mode amplitudes

$$\rho_{nm} = \sqrt{\rho_0}(R_{nm}^+ - R_{nm}^-), \quad \theta_{nm} = \frac{-i}{2\sqrt{\rho_0}}(R_{nm}^+ - R_{nm}^-). \quad (22)$$

Separating the equations and neglecting higher than second order derivatives, being small due to the large transverse size, we find that the phase fluctuations obey the same hydrodynamic equation as density fluctuations

$$\left[-\nabla_r [g_{2D}\rho_0 \nabla_r] + g_{2D}\rho_0 \frac{m^2}{r^2} \right] \frac{W_{nm}}{r^{|m|}} = \epsilon_{nm}^2 \frac{W_{nm}}{r^{|m|}} \quad (23)$$

where $\rho_{nm}(r) = \theta_{nm}(r) = r^{|m|}W_{nm}(r)$. Taking the Thomas-Fermi expression for the transverse condensate density this can be reduced to a hypergeometric equation by defining $x = r^2/b^2$:

$$\begin{aligned} x(1-x)W_{nm}'' + [(|m|+1) - (|m|+2)x]W_{nm}' \\ + \frac{\epsilon_{nm}^2 - |m|}{2}W_{nm} = 0 \quad (24) \end{aligned}$$

which has the eigenvalues and corresponding eigenstates (unnormalized)

$$\begin{aligned} \epsilon_{nm} &= \hbar\omega_r \sqrt{2n(n+m+1) + m} \quad n, m = 0, 1, 2, \dots, \\ R_{nm}(r) &= r^m \sum_{l=0}^n \frac{(n+m+l)!}{(n+m)!(m+l)!} \binom{n}{l} \left(-\frac{r^2}{b^2}\right)^l \quad (25) \end{aligned}$$

For a similar analysis of the cigar geometry, we define

$$\begin{aligned} U_n(r, z) &= \psi(r)Z_n^+(z), \quad V_n(r, z) = \psi(r)Z_n^-(z), \\ \Phi(r, z) &= \psi(r)\varphi(z) \quad \text{with } \psi(r) = \sqrt{2\beta_r} e^{-\beta_r r^2/2} \quad (26) \end{aligned}$$

and in the limit of extended axial dimension we find that the transverse density and phase fluctuations both satisfy the hydrodynamic equation

$$[-\partial_z(g_{1D}\rho_0\partial_z)]P_n(z/d) = \epsilon_n^2 P_n(z/d) \quad (27)$$

with $\rho_n(z) = \theta_n(z) = P_n(z/d)$ and an effective 1D interaction strength $g_{1D} = d^3/3$. For the Thomas-Fermi condensate density in the longitudinal direction, $P_n(z/d)$ are Legendre polynomials with eigenvalues

$$\epsilon_n = \hbar\omega_z \sqrt{\frac{1}{2}n(n+1)} \quad n = 0, 1, 2, \dots \quad (28)$$

The expressions for the normal mode energies and eigenstates in (25) and (28) are identical with results for effective 1D and 2D obtained in previous works [20, 21, 22]. However the total energy for each mode has to include the energy due to the tightly confined direction, which in effective 2D is simply $\hbar\omega_z/2$ and in 1D is $\hbar\omega_r/2$. However as the system deviates from lower dimensionality we see that contribution will change and the total energy will be

$$\begin{aligned} 2D : E_{nm} &= \frac{\hbar\omega_z}{4} \left(\beta_z + \frac{1}{\beta_z} \right) + \hbar\omega_r \sqrt{2n(n+m+1) + m} \\ 1D : E_n &= \frac{\hbar\omega_r}{2} \left(\beta_r + \frac{1}{\beta_r} \right) + \hbar\omega_z \sqrt{\frac{1}{2}n(n+1)} \quad (29) \end{aligned}$$

with $n, m = 0, 1, 2, \dots$. These expressions for the energy spectrum would apply when the system has deviated from effective lower dimensionality but has not completely attained Thomas-Fermi behavior in all directions. In this context we may point out that for a 3D cylindrically symmetric system well described by Thomas-Fermi in all dimensions, the energy spectrum is quite different from the 1D spectrum [40, 41].

Moreover the behavior of our eigenfunctions in the weakly confined dimension(s) depend on the behavior in the tightly confined dimension(s) through the interdependence of the variational parameters. Thus in the crossover regime where the β_r and β_z start to deviate significantly from unity, the shapes of the eigenmodes even in the dimension(s) of weak confinement will begin to change from what they are in effective 1D or 2D.

VI. CONCLUSION

We have developed a simple model based on a variational approach which can accurately describe the properties of a Bose Einstein condensate from the 3D Thomas-Fermi regime through various degrees of anisotropy well

into the regimes of effective 1D and 2D. The advantage of the model lies in its simplicity, so that analytic expressions could be derived for several physical quantities, and that it can explain some of the results of experiments on such systems without having to resort to complicated numerical computations.

In particular we have found expressions for the chemical potential which are valid for cylindrical condensates for all degrees of anisotropy even where the Thomas Fermi expression is completely inadequate. We have obtained expressions for the total energy and the release energy which are valid in 3D as well as in effective 1D and 2D, and the release energy was shown to agree well with experimentally measured values. Our results lead to analytic expressions for the condensate wavefunction and density, as well as the condensate dimensions for different aspect ratios in cylindrical geometry. We have also gauged the variation of the quasi-particle energy spec-

trum as the condensate deviates from effective 1D or 2D, which should provide a better estimate of spectrum-dependent physical quantities in such regimes. Our variational ansatz should be useful in studying 2D lattices of effective 1D condensates such as described in [15]; each of those 1D condensates also has an axial confinement and hence is exactly the type of high aspect ratio cigar-shaped condensates we consider here. A study of such lattices is a topic of some of our ongoing study.

It is a pleasure to acknowledge the support and help of Tom Bergeman during the initial part of this work and also valuable conversations with M. G. Moore, H. T. C. Stoof and E. M. Wright. Part of this work was done with support from ONR, and from NSF through a grant for the Institute for Theoretical Atomic and Molecular Physics at the Harvard-Smithsonian Center for Astrophysics. A later stage of the work was completed with support from ONR grant N00014-99-1-0806.

-
- [1] A. Görlitz, J. M. Vogels, A. E. Leanhardt, C. Raman, T. L. Gustavson, J. R. Abo-Shaeer, A. P. Chikkatrur, S. Gupta, s. Inouye, T. Rosenband, and W. Ketterle, *Phys. Rev. Lett.* **87**, 130402 (2001).
- [2] H. Ott, J. Fortagh, G. Schlotterbeck, A. Grossmann and C. Zimmermann, *Phys. Rev. Lett.* **87**, 230401 (2001).
- [3] A. E. Leanhardt, A. P. Chikkatrur, D. Kielpinski, Y. Shin, T. L. Gustavson, W. Ketterle, and D. E. Pritchard, *cond-mat/0203214* (2002).
- [4] A. Safonov, S. A. Vasilyev, I. S. Yasnikov, I. I. Lukashevich, and S. Jakkola, *Phys. Rev. Lett.* **81**, 4545 (1998).
- [5] B. P. Anderson and M. A. Kasevich, *Science* **282**, 1686 (1998).
- [6] L. Tonks, *Phys. Rev.* **50**, 955 (1936).
- [7] M. D. Girardeau, *J. Math. Phys.* **1**, 516 (1960)
- [8] E. Lieb and W. Liniger, *Phys. Rev.* **130**, 1605 (1963).
- [9] W. Hänsel, J. Reichel, P. Hommelhoff, and T. W. Hänsch, *Phys. Rev. Lett.* **86**, 608 (2001)
- [10] K. Bongs, S. Burger, S. Dettmer, D. Hellweg, J. Arlt, W. Ertmer, and K. Sengstock, *Phys. Rev. A* **63**, 031602 (2001).
- [11] J. Denschlag, Donatella Cassetari, and Jörg Schmiedmayer *Phys. Rev. Lett.* **82**, 2014 (1999).
- [12] M. Key, I. G. Hughes, W. Rooijackers, B. E. Sauer, and E. A. Hinds, *Phys. Rev. Lett.* **84**, 1371 (2000).
- [13] N. H. Dekker, C. S. Lee, V. Lorent, J. H. Thywissen, S. P. Smith, M. Drndić, r. M. Westervelt, and M. Prentiss, *Phys. Rev. Lett.* **84**, 1124 (2000).
- [14] J. Arlt and K. Dholakia, *Phys. Rev. A* **63**, 063602 (2001).
- [15] Markus Greiner, Immanuel Block, Olaf mandel, Theodor W. Hänsch and Tilman Esslinger *Phys. Rev. Lett.* **87**, 160405 (2001).
- [16] T. Kishimoto et al., *BAPS* **46** (No. 3), 104 (2001).
- [17] M. Olshanii, *Phys. Rev. Lett.* **81**, 938 (1998).
- [18] E. B. Kolomeisky, T. J. Newman, J. P. Straley, and Xiaoya Qi, *Phys. Rev. Lett.* **85**, 1146 (2000).
- [19] M. D. Girardeau, E. M. Wright, and J. M. Triscari *Phys. Rev. A* **63**, 033601 (2001).
- [20] D. S. Petrov, G. V. Shlyapnikov, and J. T. M. Walraven, *Phys. Rev. Lett.* **85**, 3745 (2000).
- [21] D. S. Petrov, M. Holzmann, and G. V. Shlyapnikov *Phys. Rev. Lett.* **84**, 2551 (2000).
- [22] T.-L. Ho and M. Ma, *J. Low Temp. Phys.* **115**, 61 (1999).
- [23] M. D. Girardeau and E. M. Wright *Phys. Rev. Lett.* **87**, 210401 (2001).
- [24] V. Dunjko, V. Lorent, and M. Olshanii, *Phys. Rev. Lett.* **86**, 5413 (2001).
- [25] J. O. Andersen, U. A. Khawaja, and H. T. C. Stoof, *Phys. Rev. Lett.* **88**, 070407 (2002).
- [26] U. A. Khawaja, J. O. Andersen, N. P. Proukakis, and H. T. C. Stoof, *cond-mat/0202085* (2002).
- [27] F. Dalfovo, S. Giorgini, L. P. Pitaevskii, and S. Stringari, *Rev. Mod. Phys.* **71**, 463 (1999).
- [28] F. Dalfovo, L. Pitaevskii, and S. Stringari, *Phys. Rev. A* **54**, 4213 (1996).
- [29] E. Lundh, C. J. Pethick, H. Smith, *Phys. Rev. A* **55**, 2126 (1996).
- [30] A. L. Fetter and D. L. Feder, *Phys. Rev. A* **58**, 3185 (1998).
- [31] P. Schuck and X. Vinas, *Phys. Rev. A* **61**, 043603 (2000).
- [32] B. A. McKinney and D.K. Watson, *Phys. Rev. A* **65**, 033604 (2002).
- [33] Kunal K. Das, M. D. Girardeau and E. M. Wright, *cond-mat/0204317* (2002).
- [34] G. Baym and C. Pethick, *Phys. Rev. Lett.* **76**, 6 (1996).
- [35] D. Baye and P.-H. Heenan, *J. Phys. A* **19**, 2041 (1986).
- [36] B. I. Schneider and D. L. Feder, *Phys. Rev. A* **59**, 2232 (1999).
- [37] T. Bergeman, D. Feder, N. L. Balazs, and B. Schneider, *Phys. Rev. A* **58**, 063605 (2000).
- [38] Y. Castin and R. Dum *Phys. Rev. Lett.* **77**, 5315 (1996).
- [39] P. Öhberg, E. L. Surkov, I. Tuttonen, S. Stenholm, M. Wilkens, and G. V. Shlyapnikov, *Phys. Rev. A* **56**, R3346 (1997).
- [40] M. Fliesser, A. Csordás, P. Szépfalussy, and R. Graham, *Phys. Rev. A* **56**, R2533 (1997)
- [41] S. Stringari, *Phys. Rev. A* **58** 2385 (1998)
- [42] A. L. Fetter, *Phys. Rev. A* **53**, 4245 (1996).